Engineering with Computers (2020) 36:1539–1558
https://doi.org/10.1007/s00366-019-00780-7

ORIGINAL ARTICLE

Developed comparative analysis of metaheuristic optimization algorithms for optimal active control of structures

Javad Katebi[1] · Mona Shoaei-parchin[1] · Mahdi Shariati[2] · Nguyen Thoi Trung[3,4] · Majid Khorami[5]

Received: 14 January 2019 / Accepted: 16 May 2019 / Published online: 1 June 2019

Abstract

A developed comparative analysis of metaheuristic optimization algorithms has been used for optimal active control of structures. The linear quadratic regulator (LQR) has ignored the external excitation in solving the Riccati equation with no sufficient optimal results. To enhance the efficiency of LQR and overcome the non-optimality problem, six intelligent optimization methods including BAT, BEE, differential evolution, firefly, harmony search and imperialist competitive algorithm have been discretely added to wavelet-based LQR to seek the attained optimum feedback gains. The proposed approach has not required the solution of Riccati equation enabling the excitation effect in controlling process. Employing this advantage by each of six mentioned algorithms to three-story and eight-story structures under different earthquakes led to define (1) the best solution, (2) convergence rate and (3) computational effort of all methods. The purpose of this research is to study the aforementioned methods besides the superiority of ICA in finding the optimal responses for active control problem. Numerical simulations have confirmed that the proposed controller is enabling to significantly reduce the structural responses using less control energy compared to LQR.

Keywords Active control · Metaheuristic optimization algorithm · Linear quadratic regulator (LQR) · Discrete wavelet transform (DWT)

1 Introduction

Applications of soft computing methods in different field of civil engineering have been used in many researches recently [1–14]. The idea of using active control strategy as one of these methods for civil structures has been introduced in early of 70s. The active control system can change the structural dynamic properties by adding an auxiliary input to the structure. Smart structure is the name that refers to this system [15–19].

One of the most important subjects in active control is to find out the optimum control force, so that using the least control energy, the structural responses have been remained under the allowable values [17]. Respectively, successfully implementation of the smart technology has been laid in an effective algorithm choice that adjusted the applied control forces. LQR, LQG, sliding mode control, pole assignment, H_2, and H_∞ are known as the common control algorithms [18], furthermore, LQR has been selected as the most effective, simple application and popular controller in active and semi-active structural control.

✉ Javad Katebi
jkatebi@tabrizu.ac.ir

Mona Shoaei-parchin
monashoaei@ymail.com

Mahdi Shariati
mahdishariati@duytan.edu.vn

Nguyen Thoi Trung
nguyenthoitrung@tdtu.edu.vn

Majid Khorami
majid.khorami@ute.edu.ec

1 Faculty of Civil Engineering, University of Tabriz, Tabriz 51666-16471, Iran

2 Institute of Research and Development, Duy Tan University, Da Nang 550000, Vietnam

3 Division of Computational Mathematics and Engineering, Institute for Computational Science, Ton Duc Thang University, Ho Chi Minh City, Vietnam

4 Faculty of Civil Engineering, Ton Duc Thang University, Ho Chi Minh City, Vietnam

5 Facultad de Arquitectura y Urbanismo, Universidad UTE, Calle Rumipamba s/n y Bourgeois, Quito, Ecuador

The objective of LQR is to minimize a quadratic cost function establishing a reasonable balance between the reduction of responses and required control forces. During the minimization procedure, the external excitation has not participated in solving the Riccati algebraic equation avoiding LQR as truly optimal. An applicable solution to deal with the mentioned difficulties has been passed through the intelligent optimization methods. The metaheuristic capabilities in the global optimal solution achievement for nonlinear and complex problems have provided a lot of flexibility in design controller.

Electrical and mechanical engineering have proposed multi-objective approaches for selecting LQR weights in controlling of double-inverted pendulum system [20]. Wang et al. [21] has applied Artificial Bee Colony (ABC) algorithm in weight selection of LQG for large antenna servo, and to avoid the repeated adjustment of LQR weights, accordingly, ABC has been used to determine Q and R for inverted pendulum system [22].

According to the literature, few studies have been performed in structural control as well as LQR weight selection based on metaheuristic algorithms. GA as an effective optimization technique has been used for LQR weighting matrix selection [23–31]. In the field of active and passive control design, GA has been used successfully for response mitigation of coupled buildings [16], finding the optimal size and location of passive devices [32, 33], number and location of active control devices and sensors [17, 34]. Joghataie and Mohebbi [26] have proposed an optimal control algorithm based on nonlinear Newmark integration and distributed genetic algorithm (DGA) used to optimally select weights in the proposed controller. Amini et al. [35] has presented a method to find the optimal control forces for active tuned mass damper. In this research, to eliminate the trial and error, particle swarm optimization (PSO) has been used to determine feedback gains with online updates of LQR weighting matrices. To optimize the number, location and total driving force of required actuators, an improved particle swarm algorithm has been presented in [36]. Amini and Ghaderi [37] have described an improved version of ant colony optimization (ACO) to find the optimal locations of fuzzy logic-controlled MR dampers. Harmony search (HS) has been utilized in the field of structural control as well as in [38]. Hybridization of HS and ACO for optimal locating of dampers has been discussed in [39], and a comprehensive review of the researches on the optimal damper location problem based on optimization algorithms has been presented in [40]. Several attempts have been made to determine the optimal parameters of the tuned mass damper (TMD) via metaheuristic algorithms. Mohebbi and Joghataie [41] have developed a DGA-based control algorithm for minimizing these parameters. Few researchers [35, 42–45] have used an improved version of PSO for optimizing the required parameters of TMD. Leung and Zhang [46] have also used an improved version of PSO for optimizing the required parameters of TMD. Differential evolution (DE) algorithm has been applied to obtain optimum parameters of passive device by minimizing H_2 and H_∞ norms of the benchmark system equipped with TMD [47]. Bagheri and Amini [48] have proposed the controller employing the pattern search method in minimizing LQR performance index. Amini and Bagheri [49] have presented an approach for the optimal control of structures estimating the control forces conducted by the performance index optimization through the colonial competitive algorithm.

As mentioned earlier, those studies applied metaheuristics involved in the field of seeking the optimal number and location of sensors and actuators, setting the parameters of passive TMD systems and selecting the LQR weighting matrices for active control systems [27–29, 31, 50–55]. However, few studies have been conducted in active control problem focusing on the classical methods' shortcoming such as sub-optimality problem and the effect of external excitation in control forces calculation. On the other hand, some of metaheuristics have not been explored in control problem yet.

In this research, wavelet transform is used to decompose the external excitation into different frequency bands, thus the elements of feedback gain matrix are searched by six optimization techniques in each frequency range. Achieving the best solution, convergence rate and computational effort of these algorithms are compared through two numerical examples:

- imperialist competitive algorithm (ICA) as a socio-politically motivated algorithm,
- differential evolution (DE) as an evolutionary method,
- BAT, BEE and firefly (FA) as natural-inspired algorithms, and
- harmony search (HS) as music-inspired metaheuristic.

According to the knowledge of the authors, this comparison has not discussed the structural active control problem yet; therefore, the formulation has not required the solution of Riccati algebraic equation and could regard the external excitation effect.

The current study has focused on the state space equation of motion and formulation of LQR control problem, followed by outlining the proposed approach, respectively, first wavelet transform is briefly introduced and the metaheuristics' usage in wavelet-based LQR controller has been detailed. Also, the model structures and used earthquakes are introduced; furthermore, an overview on components and operators of metaheuristics has been demonstrated to present and compare the simulation results.

2 System equations and linear quadratic regulator

A review of performed studies in structural control has shown the efficiency and applicability of LQR making it the most popular control techniques. For a building equipped with an active tendon control subjected to a ground excitation, the state space description of system motion is expressed as follows:

$$\dot{X}(t) = AX(t) + BU(t) + E\ddot{X}_g(t), \tag{1}$$

$X(t) = \left[q(t), \dot{q}(t)\right]^T$ is called the state vector, where $q(t)$ and $\dot{q}(t)$ denote the n-dimensional vector of the relative displacements and velocities. A (plant matrix), B (control matrix) and E (excitation matrix) are given by the following equations:

$$A = \begin{bmatrix} O & I \\ -M^{-1}K_s & -M^{-1}C_d \end{bmatrix}_{2n\times 2n}, \tag{2}$$

$$B = \begin{bmatrix} O \\ M^{-1}H \end{bmatrix}_{2n\times n}, \tag{3}$$

$$E = \begin{bmatrix} O \\ -M^{-1}\Gamma \end{bmatrix}_{2n\times n}, \tag{4}$$

where M, C_d and K_s are $n \times n$ matrices of mass, damping and stiffness of the structure, respectively, $U(t)$ is $m \times 1$ control force vector applied by m actuators and $\ddot{X}_g(t)$ representing the time history of ground acceleration. Γ is $n \times 1$ influencing vector of the external forces and H is defined as $n \times m$ location matrix of actuators.

Due to the actuator capacity curbs and economic efficiency, the response mitigation under allowable values with less control energy is desirable. The linear quadratic regulator is a minimized quadratic performance index to make a good trade-off between limiting the structural response and reducing the control force consumption. This quadratic performance index "J" is formulated as follows:

$$J = \int_{t_0}^{t_f} [X(t)^T QX(t) + U(t)^T RU(t)]\mathrm{d}t, \tag{5}$$

where Q and R are referred to state and control force weighting matrices and tf is the duration of earthquake. Essentially, Q is non-negative semi-definite and R is the positive definite matrices. The solution has been provided by the feedback control law and the control force calculated by the following equation based on the system's states:

$$\{U(t)\}_{n\times 1} = -[K]_{n\times 2n}\{X(t)\}_{2n\times 1}, \tag{6}$$

where K is the feedback gain matrix (Eq. 7) and the symmetric matrix P is the solution of algebraic Riccati equation (ARE):

$$K = -R^{-1}B^T P, \tag{7}$$

$$A^T P + PA - PBR^{-1}B^T P + Q = -\dot{P}. \tag{8}$$

3 Wavelet-based optimal active control formulation

The wavelet transform (WT) as one of the most effective time–frequency analysis tools can be used to detect the local frequency content of earthquakes. WT is a transformation decomposing the signal into a superposition of the elementary basic function $\psi_{s,\tau}(t)$ called mother wavelet. The wavelets are generated from scaling and translation of this mother wavelet. The continuous wavelet transform (CWT) of the signal $x(t)$ is expressed as

$$wt(s,\tau) = \frac{1}{\sqrt{s}}\int_{-\infty}^{+\infty} x(t)\psi^*\left(\frac{t-\tau}{s}\right)\mathrm{d}t, \tag{9}$$

where ψ^* is the complex conjugation of ψ and wt (s,τ) is called the wavelet coefficient. In Eq. (9), s is the scale factor representing the frequency content of signal and translation factor τ discriminating the location of wavelets during the time. The discrete version of wavelet transform (DWT) has been used by discretizing the scale and translation parameter. Using dyadic values for τ and s (Eq. 10), the corresponding $wt_{j,k}(t)$ is as Eq. (11). j and k are positive integers.

$$s = 2^{-j}, \quad \tau = 2^{-j}k, \tag{10}$$

$$wt_{j,k}(t) = 2^{j/2}\psi(2^j t - k). \tag{11}$$

If the earthquake signal $\ddot{x}_g(t)$ is decomposed to I level using DWT:

$$\ddot{x}_g(t) = A_I(t) + \sum_{i\le I} D_i(t), \tag{12}$$

D_i is the ith detail and A_I is the Ith level of approximate signal. Adopting this approach, LQR performance index has been computed as follows:

$$X_i(t) = \left[q_i(t), \dot{q}_i(t)\right], \tag{13}$$

$$X_I(t) = \left[q_I(t), \dot{q}_I(t)\right], \tag{14}$$

$$\begin{aligned} J = &\int_0^{t_f} [X_I(t)^T Q\, X_I(t) + U_I(t)^T RU_I(t)]\mathrm{d}t \\ &+ \sum_{i\le I}\int_0^{t_f} [X_i(t)^T Q\, X_i(t) + U_i(t)^T RU_i(t)]\mathrm{d}t, \end{aligned} \tag{15}$$

$$X = X_I(t) + \sum_{i \le I} X_i(t), \tag{16}$$

$$U = U_I(t) + \sum_{i \le I} U_i(t). \tag{17}$$

In this study, to enhance the controller performance, DWT has been applied to decompose the excitation into different frequency bands. For decomposition process, signal is decomposed using Daubechies wavelet of order 10 (db 10) mother wavelet in five levels.

Defined wavelet-based performance index (Eq. 15) has been selected as objective function and gain matrix elements considered as design variables of optimization process. Then metaheuristic algorithm has been employed to search the optimum gain matrix for each frequency band to calculate the control force in each domain (Eq. 18), thus total control force is also calculated with Eq. (19). K_i is the gain matrix at level i.

$$\begin{aligned} U_I(t) &= -K_I X_I(t), \\ U_i(t) &= -K_i X_i(t), \end{aligned} \tag{18}$$

$$U(t) = -K_I X_I(t) - \sum_{i \le I} K_i X_i(t). \tag{19}$$

Adopting this approach, the earthquake excitation has been participated in solving the Riccati equation and calculating the control forces. The proposed controller has been employed by different optimization algorithms to increase the accuracy toward the optimum controller gains comparing different aspects of metaheuristics in dealing with the optimal active control problem.

According to the results of this study, the effectiveness of each algorithm in vibration reduction through various seismic excitations has been evaluated by numerical simulations. This formula is able to be easily performed with any metaheuristic algorithm providing the great flexibility in the active controller design (Fig. 1).

4 Numerical study

To investigate the performance of proposed controller, three- and eight-story shear frames have been equipped with active tendon system selected as numerical examples. The schematic model of mentioned structures and dynamical properties of these structures are summarized in Table 1 and Fig. 2. The placed actuators in all stories have applied the control force.

The displacement response of structure's upper story (Fig. 2) was calculated by earthquake excitation (Fig. 3) for uncontrolled and controlled structures, and required control forces were obtained. Then the performance of each controller has been evaluated in terms of reducing the displacement response and the required control force compared to uncontrolled mode. Finally, the advantages of different optimization algorithms are compared in optimized controller design from a variety of aspects. Comparing the performance of the controller in addition to the structure response, nine indicators of performance in Table 2 have been used for more accurate comparison.

The time history of the earthquake records is introduced as the input of the system and the velocity and displacement responses of the structure is received as the output of the program. Based on the output values and using control rule, Eq. 19 of the time history of the control forces applied to the structure was calculated.

To demonstrate the effectiveness and potential application of controller for different earthquakes, aforementioned structures are analyzed under three well-known historical earthquakes: Kobe (PGA = 0.345 g), Landers (PGA = 0.245 g) and Parkfield (PGA = 0.357 g) ground motions. The details of the earthquakes are shown in Fig. 3.

In addition to wavelet-based LQR performance index used as objective function of optimization, nine benchmark indices obtained from the results are calculated (Table 2) to evaluate the controller performance by reduction of different design parameters such as interstory drift, story displacement, acceleration, base shear and needed control force compared to the uncontrolled cases.

$d_i(t)$, $x_i(t)$, $\ddot{x}(t)$, h_i and m_i are the interstory drift, displacement, acceleration, height and mass of the ith story, respectively. $f_l(t)$ is the control force produced by lth actuator and W is the structure weight. c and uc superscripts are related to controlled and uncontrolled cases.

In the following, the basic steps of aforementioned intelligent optimization methods are expressed as pseudo-code (a brief review on the operators and parameters of metaheuristic algorithm). Then the controller based on these algorithms is applied to the prior structures under various earthquakes and the performance of the optimal smart systems is compared to the uncontrolled one, LQR controller and one another.

4.1 The ICA-based optimal controller

Imperialist competitive algorithm inspired by imperialist competition has been developed by Atashpaz-Gargari and Lucas [57]. The pseudo-code of ICA is shown in Fig. 4.

ICA has required specific parameters to effectual performance affecting the quality of results and algorithm capability. In this study, ICA parameters are set as in Table 3

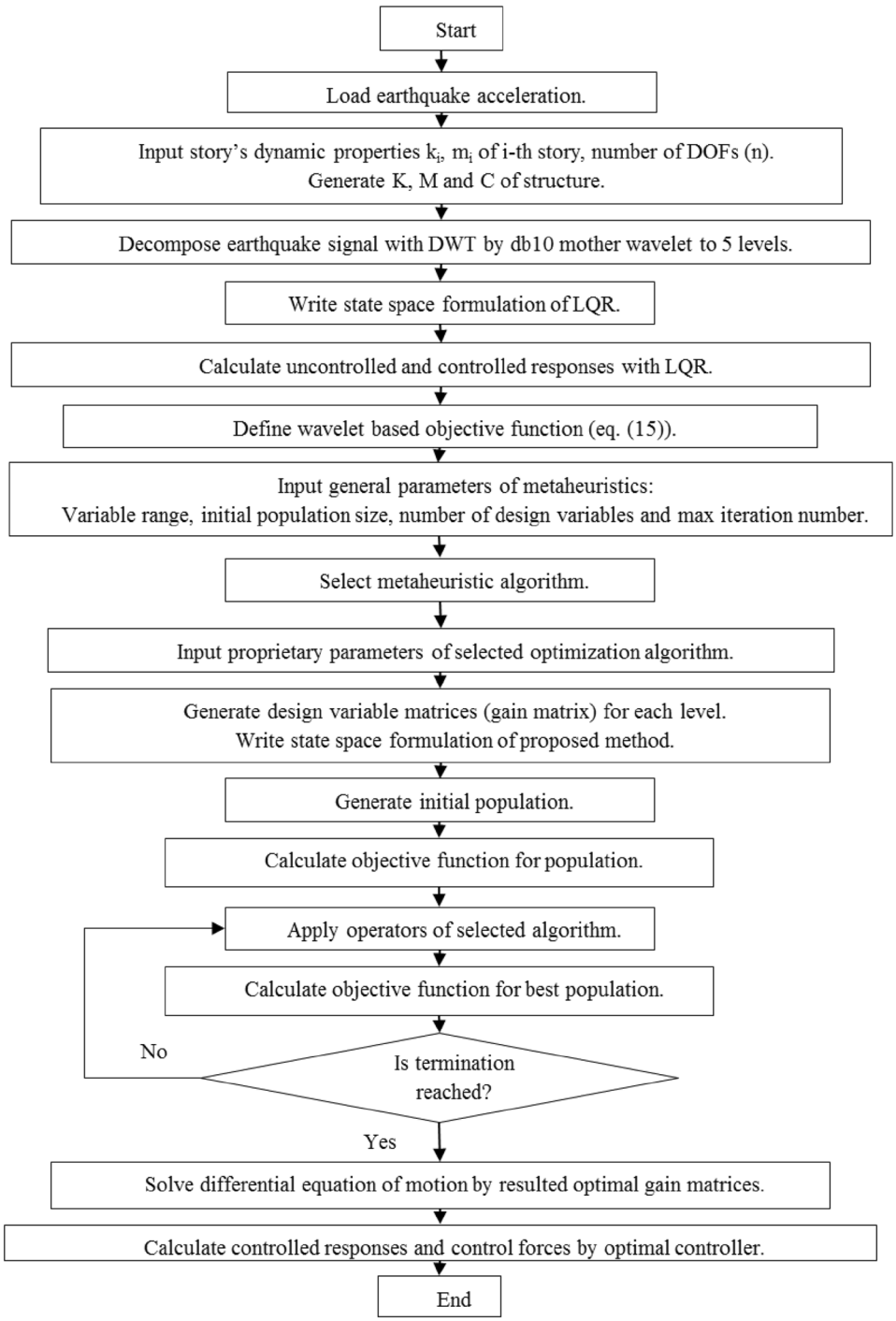

Fig. 1 The flowchart of proposed optimal controller

Table 1 Dynamical properties of studied structures

	m_i (ton)	k_i (kN/m)	c_i (kN s/m)	ζ_i
3-dof	1	980	1.407	$\zeta = 0.01, 0.028, 0.04$
8-dof	345.6	680,000	734	$\zeta = 0.004, 0.013, 0.021, 0.028, 0.035, 0.04, 0.044, 0.047$

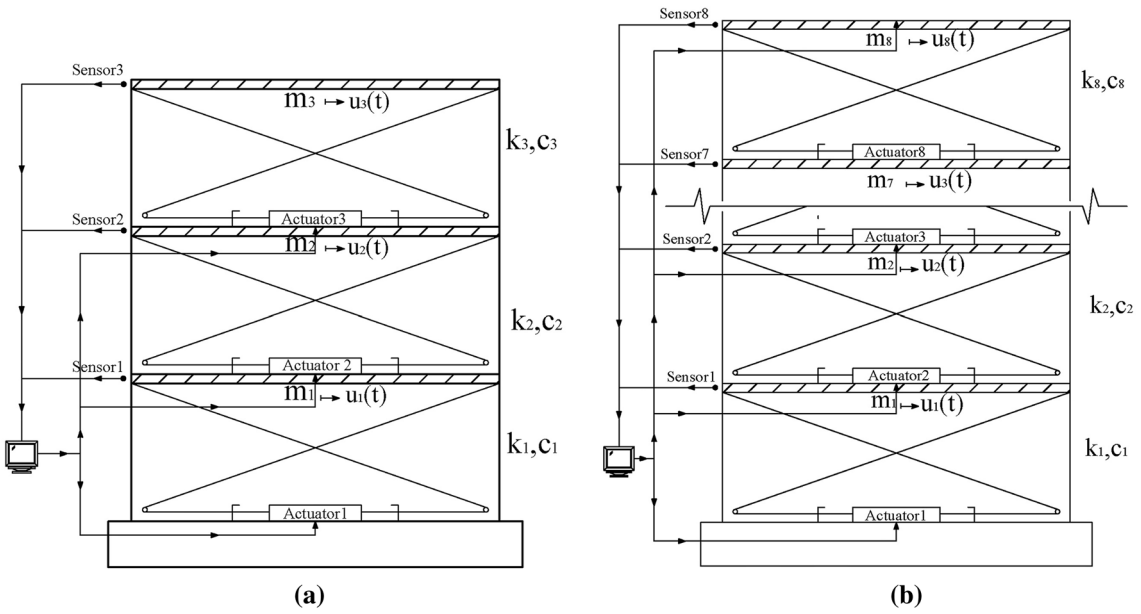

Fig. 2 Aforementioned structures equipped with active tendons: **a** 3-dof; **b** 8-dof structures

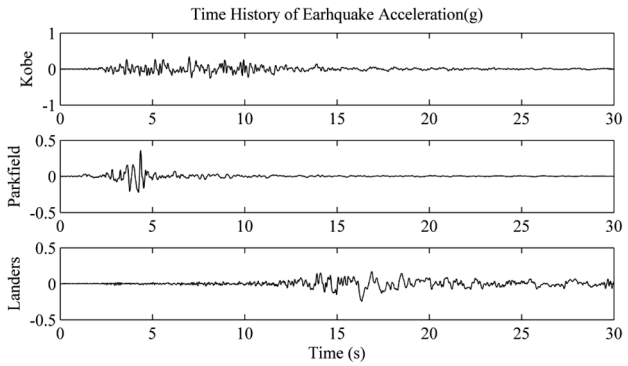

Fig. 3 The time histories of Kobe, Parkfield and Landers earthquakes

The maximum number of iterations has been selected based on the required accuracy of optimization; accordingly, in this study, 50 iterations have been selected for ICA. The process has started to solve vibration control problems with 30 (for 3-dof structure) and 50 (for 8-dof structure) population size. In the following, ICA's performance in confronting with active control problem has been studied by numerical simulations.

Table 3 The values of ICA parameters

Number of imperialists	N_{imp}	3
Revolution rate	R	0.3
Assimilation coefficient	β	2
Assimilation angular coefficient	γ	0.5

Table 2 Formulas of benchmark indices [56]

Interstory drift ratio	Level displacement	Level acceleration	Base shear
$J_1 = \dfrac{\max\limits_{t,i} \frac{\lvert d_i^c(t)\rvert}{h_i}}{\max\limits_{t,i} \frac{\lvert d_i^{uc}(t)\rvert}{h_i}}$	$J_2 = \dfrac{\max\limits_{t,i} \lvert x_i^c(t)\rvert}{\max\limits_{t,i} \lvert x_i^{uc}(t)\rvert}$	$J_3 = \dfrac{\max\limits_{t,i} \lvert \ddot{x}_{ai}^c(t)\rvert}{\max\limits_{t,i} \lvert \ddot{x}_{ai}^{uc}(t)\rvert}$	$J_4 = \dfrac{\max\limits_{t} \lvert \sum_i m_i \ddot{x}_{ai}^c(t)\rvert}{\max\limits_{t} \lvert \sum_i m_i \ddot{x}_{ai}^{uc}(t)\rvert}$
Normed interstory drift ratio	**Normed level displacement**	**Normed level acceleration**	**Normed base shear**
$J_5 = \dfrac{\max\limits_{t,i} \frac{\lVert d_i^c(t)\rVert}{h_i}}{\max\limits_{t,i} \frac{\lVert d_i^{uc}(t)\rVert}{h_i}}$	$J_6 = \dfrac{\max\limits_{t,i} \lVert x_i^c(t)\rVert}{\max\limits_{t,i} \lVert x_i^{uc}(t)\rVert}$	$J_7 = \dfrac{\max\limits_{t,i} \lVert \ddot{x}_{ai}^c(t)\rVert}{\max\limits_{t,i} \lVert \ddot{x}_{ai}^{uc}(t)\rVert}$	$J_8 = \dfrac{\max\limits_{t} \lVert \sum_i m_i \ddot{x}_{ai}^c(t)\rVert}{\max\limits_{t} \lVert \sum_i m_i \ddot{x}_{ai}^{uc}(t)\rVert}$
Control force			
$J_9 = \dfrac{\max\limits_{t,i} \lvert f_i(t)\rvert}{W}$			

Imperialist Competitive Algorithm

Begin
Objective function f(x), $\boldsymbol{x} = (x_1, \ldots, x_d)^T$;
Generate initial population (countries) randomly $\boldsymbol{x_i}$ (i = 1, 2, ..., n);
Define number of imperialists (Nimp), Revolution rate (R), Assimilation coefficient (β) and Assimilation angular coefficient (γ)
Initialize algorithm by evaluating the fitness of each country
The most powerful countries is selected as the imperialists and Other countries as colonies allocated to imperialists based on their power
while *(t <Max number of iteration)*
Generate new solutions by applying assimilation operator; Colonies move towards Imperialist's states from different directions
updating position of countries by Revolution: Random changes occur in the characteristics of countries
if *$f(imp_i) > f(colony_i)$*
Swap positions of the imperialist and colony
Compute the total cost of all empires (Related to the power of both imperialist and its colonies).
end if
Imperialistic competition: All imperialists compete to take possession of colonies of each other.
Eliminate the powerless empires. Weak empires lose their power gradually and they will finally be eliminated.
end while
Post process results and visualization;
End

Fig. 4 The pseudo-code of ICA

4.1.1 Vibration control of structures with ICA-based optimal controller

In example 1, the responses of 3-dof building are controlled. The needed control force and controlled displacement of top story due to Kobe earthquake are presented with the corresponding uncontrolled ones in Fig. 5. The comparative results are drawn in Table 4.

On the whole, the results have shown that ICA controller can find more optimal objective function than LQR. The maximum displacement of 3-dof roof under Kobe earthquake has been reduced 11% with only 91% of maximum

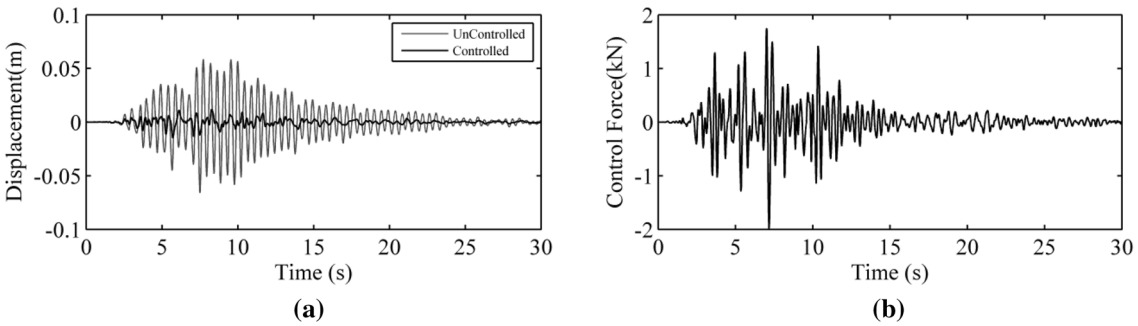

Fig. 5 The results of ICA controller for 3-dof's top story under Kobe earthquake: **a** displacement; **b** control force

Table 4 The comparison between ICA and LQR for 3-dof under Kobe earthquake

	J	Maximum displacement of top story (Dispmax) (m)	Maximum velocity of top story (Velmax) (m/s)	Maximum acceleration of top story (Accmax) (m/s^2)	Maximum control force of top story (Umax) (kN)	Maximum drift of structure (Driftmax)
Uncontrol (UC)	–	0.0658	0.9369	15.7387	–	0.00468
LQR	0.4956	0.0164	0.2573	5.3770	2.1641	0.00381
ICA	0.4384	0.0146	0.2208	4.7267	1.9820	0.00124

Table 5 Comparison between ICA and LQR for 8-dof under Parkfield earthquake

	J	Dispmax (m)	Velmax (m/s)	Accmax (m/s^2)	Umax (kN)	Driftmax
UC	–	0.0375	0.4303	7.3899	–	0.0011
LQR	1.2295	0.0205	0.2326	4.5455	576.798	0.0005
ICA	1.0794	0.0203	0.2708	5.5173	285.469	0.0006

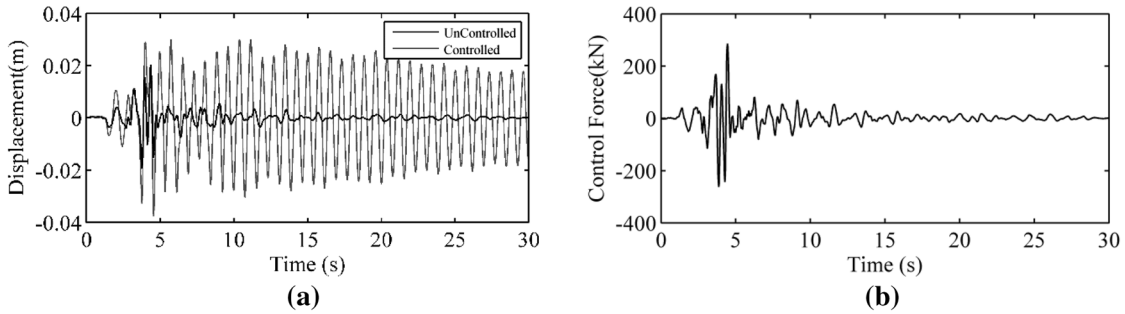

Fig. 6 Results of ICA controller for 8-dof's top story under Parkfield earthquake: **a** displacement; **b** control force

Differential Evolution Algorithm

Begin
*Objective function f (**x**), **x** = (x$_1$, ..., xd)T*
*Generate initial population of individuals **x**$_i$(i = 1, 2, ..., n)*
Calculate the fitness of the initial population.
Define Scale coefficient (F) and Crossover probability (CR)
***while** (t <MaxGeneration)*
***for j**= 1 : **n** all **n** individuals (each individual j in the population)*
Choose three numbers n1,n2, n3 that is 1≤n1,n2, n3 ≤N with n1≠n2 ≠n3≠j
Generate a random integer i rand(1, N)
for i
Create mutant vector y=n3+F.(n1-n2)
z=y if rand()≤CR or j=j$_{rand}$
x otherwise
end for
***if** (f(z)≤f(x))*
x=z
end if
end for
Rank the individuals and find the best
end while
Post process results and visualization;
End

Fig. 7 The pseudo-code of DE

Table 6 The values of DE parameters

Scale coefficient	F	0.5
Crossover probability	CR	0.2

control force needed for LQR. Maximum drift, acceleration and velocity have also been reduced by ICA controller. According to Table 5, the maximum displacement of 8-dof roof under Parkfield earthquake is approximately the same as LQR with only using of 50% of maximum control force (Fig. 6).

4.2 The DE-based optimal controller

Differential evolution algorithm has been proposed by Storn and Price [58]. The main concepts of DE are shown in the pseudo-code given in Figure 7

The parameters shown in Table 6 are considered for DE, in this paper (Fig. 8).

4.2.1 Vibration control of structures with DE-based optimal controller

The results of structural displacement and control force for 8-dof top story due to Parkfield earthquake calculated by DE controller are shown in Fig. 9.

The results have indicated that DE controller has reduced both the displacement and control forces simultaneously for 3-dof and 8-dof (Tables 7, 8).

4.3 BAT-based optimal controller

The standard BAT algorithm has been introduced by Xin-She Yang [51] based on the echolocation behavior of microbats to find and hunt for prey. The procedure of BAT is shown through the stages in pseudo-code (Fig. 10).

In this paper, to solve the optimal active control problem, the parameters of Table 9 have been selected for BAT algorithm; therefore, the related subsection has presented the results of BAT-based controller to studied structures.

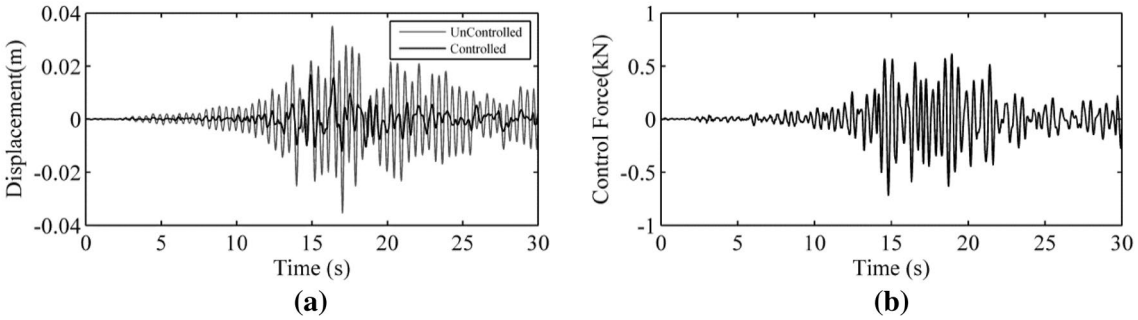

Fig. 8 Results of DE controller for 3-dof top story under Landers earthquake: **a** displacement; **b** control force

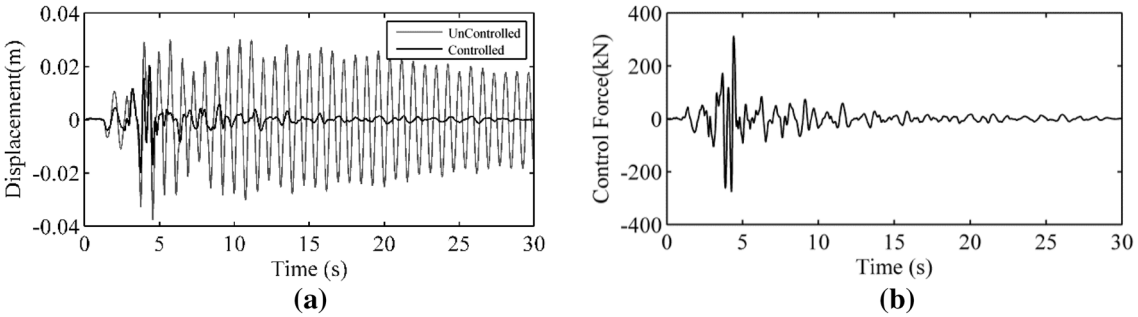

Fig. 9 Results of DE controller for 8-dof top story under Parkfield earthquake: **a** displacement; **b** control force

Table 7 Comparison between DE and LQR for 3-dof under Landers earthquake

	J	Dispmax (m)	Velmax (m/s)	Accmax (m/s^2)	Umax (kN)	Driftmax
UC	–	0.0354	0.4424	6.8714	–	0.0024
LQR	0.3248	0.0189	0.1771	2.2658	1.125	0.0011
DE	0.28	0.0168	0.1784	2.6674	0.72	0.0011

Table 8 Comparison between DE and LQR for 8-dof under Parkfield earthquake

	J	Dispmax (m)	Velmax (m/s)	Accmax (m/s^2)	Umax (kN)	Driftmax
UC	–	0.0375	0.4303	7.3899	–	0.00217
LQR	1.2295	0.0205	0.2326	4.5455	576.7981	0.00133
DE	1.1781	0.0204	0.2834	5.8792	312.1668	0.00141

4.3.1 Vibration control of structures with BAT-based optimal controller

The 8-dof's displacement and control force in the cases of uncontrolled, LQR and BAT controller are presented in Fig. 12 and Table 11.

According to Figs. 11 and 12, and Tables 10 and 11, this controller has performed better than conventional LQR in reducing the displacements and control force for 3-dof and 8-dof structures.

4.4 The BEE-based optimal controller

In this study, BEE algorithm [59] (as fourth metaheuristic technique) has been used as an optimization algorithm inspired by the natural foraging behavior of honey bees to find the food resources. Pseudo-code of this algorithm is drawn in Fig. 13.

The algorithm required the number of parameters as in Table 12.

The time history of displacement response and control force for 3-dof shear frame under Landers earthquake is shown in Fig. 14. Also, Fig. 15 shows the time history of

Fig. 10 The pseudo-code of BAT algorithm

BAT Algorithm

Begin
Objective function f(x), $\boldsymbol{x} = (x_1, \ldots, x_d)^T$;
Initialize the bat population $\boldsymbol{x}_i$ $(i = 1, 2, \ldots, n)$;
Define pulse frequency $\boldsymbol{f}_i$ *at* $\boldsymbol{x}_i$ *position with* $\boldsymbol{v}_i$ *velocity*
Initialize pulse rate $\boldsymbol{r}_i$ *and the loudness* $\boldsymbol{A}_i$
while $(t <$*Max number of iteration*$)$
Generate new solutions by adjusting frequency and updating velocities and locations/solutions;
if $(\boldsymbol{rand} > \boldsymbol{r}_i)$
select a solution among the best solutions
Generate a local solution around the selected best solution;
end if
Generate a new solution by flying randomly
if $(\boldsymbol{rand} < \boldsymbol{A}_i \,\&\, \boldsymbol{f}(\boldsymbol{x}_i) < \boldsymbol{f}(\boldsymbol{x}_*))$
Accept the new solutions
Increase $\boldsymbol{r}_i$ *and reduce* $\boldsymbol{A}_i$
end if
Rank the bats and find the current best $\boldsymbol{x}_*$
end while
Post process results and visualization;
End

Table 9 The values of BAT parameters

Minimum frequency	$f_{\min}$	0
Maximum frequency	$f_{\max}$	1
Loudness	A	0.5
Pulse emission rate	r	0.5

response and needed control force for 8-dof excited by Parkfield earthquake.

4.4.1 Vibration control of structures with BEE-based optimal controller

BEE has outstandingly performed LQR in terms of controller effort and structural responses (Tables 13, 14).

4.5 FA-based optimal controller

The firefly algorithm (FA) has been developed by Xin-She Yang [60] based on the idealization of flashing characteristics of fireflies. The firefly's behavior is modeled to develop FA by the following process (Fig. 16).

In this study, the values shown in Table 15 are considered for FA parameters.

4.5.1 Vibration control of structures with FA-based optimal controller

The simulation results of 3-dof and 8-dof structures subject to the Parkfield earthquake calculated by FA controller have been sketched in Figs. 17 and 18.

Table 10 Comparison between BAT and LQR for 3-dof under Parkfield earthquake

	J	Dispmax (m)	Velmax (m/s)	Accmax (m/s^2)	Umax (kN)	Driftmax
UC	–	0.05443	0.8403	13.3886	–	0.003515
LQR	0.5793	0.0269	0.4847	7.4851	2.2456	0.002106
BAT	0.4416	0.0239	0.4378	7.0013	1.7225	0.001947

Table 11 Comparison between BAT and LQR for 8-dof under Parkfield earthquake

	J	Dispmax (m)	Velmax (m/s)	Accmax (m/s^2)	Umax (kN)	Driftmax
UC	–	0.0375	0.4303	7.3899	–	0.0011
LQR	1.2295	0.0205	0.2326	4.5455	576.798	0.0005
BAT	1.1993	0.0198	0.2717	5.8573	427.913	0.0007

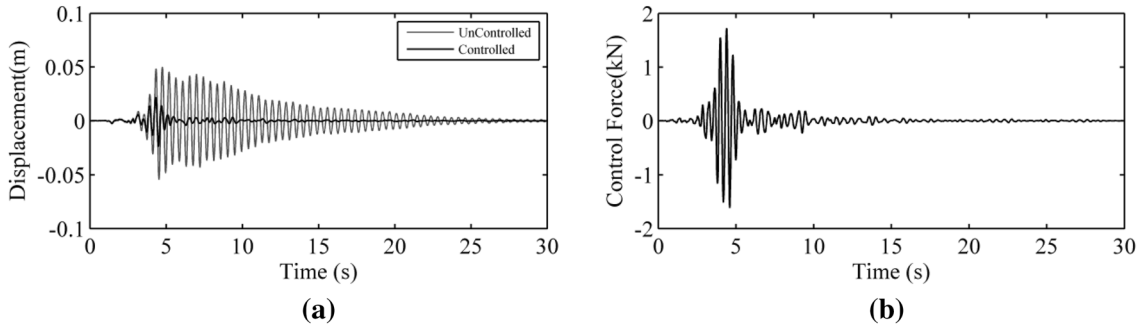

Fig. 11 The results of BAT controller for 3-dof top story under Parkfield earthquake: **a** displacement; **b** control force

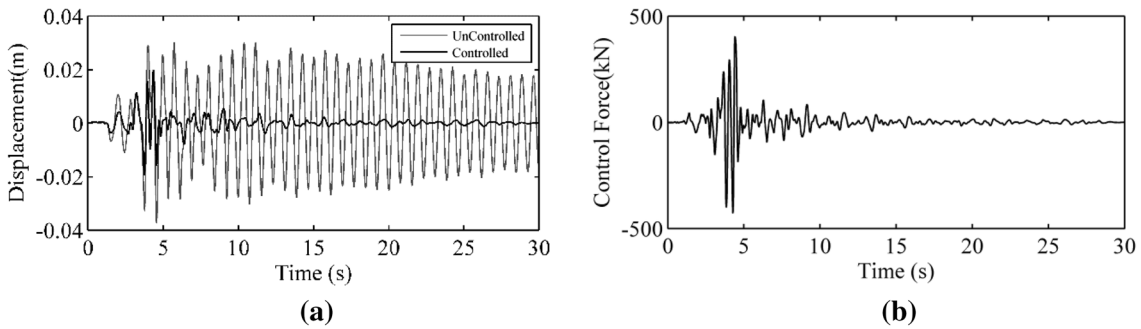

Fig. 12 The results of BAT controller for 8-dof top story under Parkfield earthquake: **a** displacement; **b** control force

BEE Algorithm

Begin
*Objective function f (**x**), **x** = $(x_1, ..., x_d)^T$;*
Generate initial population of bees $\mathbf{x}_i$ (i = 1, 2, ..., n)
Evaluate fitness of the population
Define Number of selected sites (m), Number of best sites (e), Number of bees recruited for best sites (nep) and Number of bees recruited for other sites (nsp)
***while** (t <MaxGeneration)*
***for i** = 1 : **n** all **n** bees*
Select e Elite patches from m patches
Assign nep bees per elite patch
Evaluate the fitness function of the nep bees
Sort the results based on their fitness, Select the fittest patch
Select m-e Best patches
Assign nsp bees per best patch
Evaluate the fitness function of the nsp bees
Select the fittest patch
end for
random search
Evaluate the fitness function of the random solutions
Create new population
Rank the bees and find the current best
end while
Post process results and visualization;
End

Fig. 13 The pseudo-code of BEE algorithm

Table 12 The values of BEE parameters

Number of sites selected	m	15
Number of best sites	e	6
Number of bees recruited for best sites	nep	30
Number of bees recruited for the other sites	nsp	15

The proposed controller has reduced the maximum displacement and control force for 3-dof and 8-dof structures (Tables 16, 17).

4.6 The harmony search-based optimal controller

Geem et al. [61] has pioneered harmony search (HS) by seeking harmony in music making. The following pseudo-code has shown how the harmony in music has inspired finding an optimality in an optimization problem (Fig. 19). HS parameter setting is shown in Table 18.

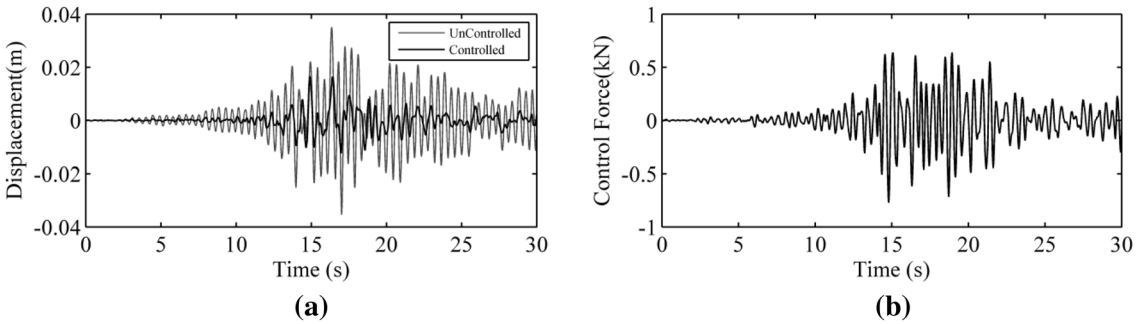

Fig. 14 Results of BEE controller for 3-dof top story under Landers earthquake: **a** displacement; **b** control force

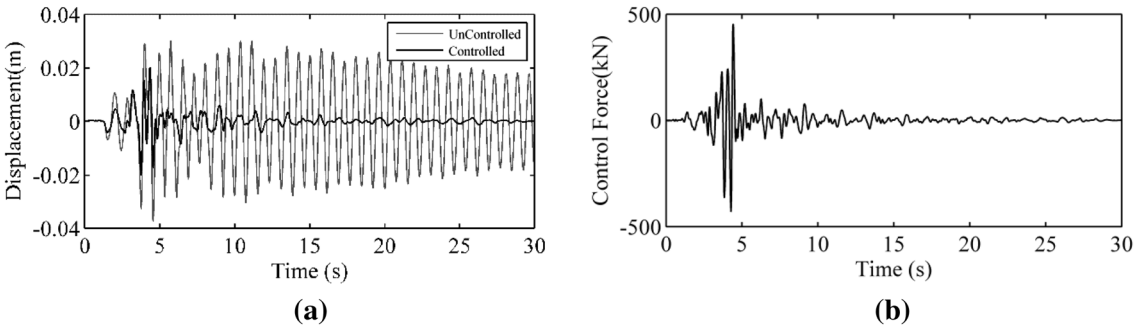

Fig. 15 Results of BEE controller for 8-dof top story under Parkfield earthquake: **a** displacement; **b** control force

Table 13 Comparison between BEE and LQR for 3-dof under Landers earthquake

	J	Dispmax (m)	Velmax (m/s)	Accmax (m/s^2)	Umax (kN)	Driftmax
UC	–	0.0354	0.4424	6.8714	–	0.0024
LQR	0.3248	0.0189	0.1771	2.2658	1.125	0.0011
BEE	0.2827	0.0165	0.178	2.6529	0.771	0.0011

Table 14 Comparison between BEE and LQR for 8-dof under Parkfield earthquake

	J	Dispmax (m)	Velmax (m/s)	Accmax (m/s^2)	Umax (kN)	Driftmax
UC	–	0.0375	0.4303	7.3899	–	0.0011
LQR	1.2295	0.0205	0.2326	4.5455	576.798	0.0005
BEE	1.2895	0.0203	0.2852	6.1476	453.94	0.0007

Firefly Algorithm

Begin
*Objective function f (**x**), **x** = $(x_1, ..., x_d)^T$;*
Generate initial population of fireflies $\mathbf{x}_i$ (i = 1, 2, ..., n)
Light intensity $\mathbf{I}_i$ at $\mathbf{x}_i$ is determined by f (x_i)
*Define light absorption coefficient **γ***
***while** (t <MaxGeneration)*
***for i** = 1 : **n** all **n** fireflies*
***for j** = 1 : **i** all n fireflies (inner loop)*
***if** ($\mathbf{I}_j > \mathbf{I}_i$)*
*Move firefly **i** towards **j** ;*
end if
*Attractiveness varies with distance **r** via $\mathbf{e}^{-\gamma r}$*
Evaluate new solutions and update light intensity
end for j
end for i
Rank the fireflies and find the current best
end while
Post process results and visualization;
End

Fig. 16 The pseudo-code of firefly algorithm

Table 15 The values of FA parameters

Randomization parameter	α	0.5
Attractiveness	β	0.2
Light absorption coefficient	γ	1

4.6.1 Vibration control of structures with HS-based optimal controller

HS is also utilized to solve the numerical examples. The simulation results are depicted in Figs. 20 and 21.

According to the results, HS controller has reduced the third floor displacement more than 13% compared to LQR. Simultaneously, the applied control force is reduced to 89% (Table 19).

The maximum displacement of the eighth story is reduced from 35 mm in the uncontrolled case to 20 mm in LQR and HS, also the maximum of needed control force for HS controller is 216 kN less than LQR (Fig. 21 and Table 20). The results have represented the power of metaheuristics and superiority of these controllers over the classical LQR in controlling the vibration of 3-dof and 8-dof structures subjected to different earthquake excitations. The next section has contained the results comparing different aspects of studied metaheuristics in dealing with active control problem.

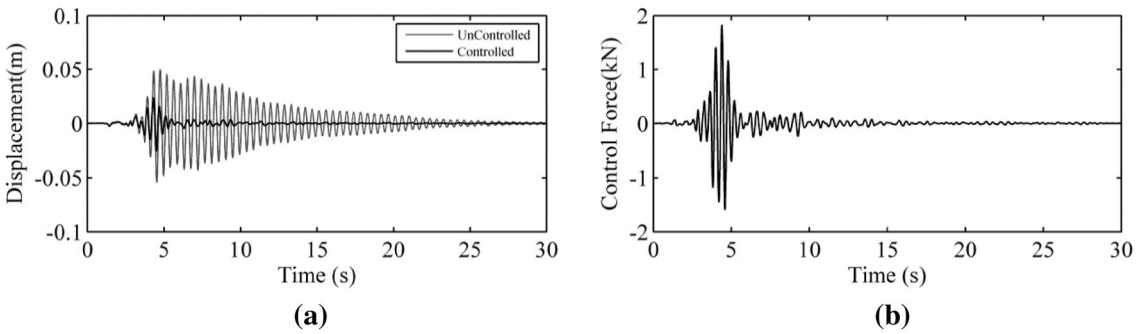

Fig. 17 Results of FA controller for 3-dof top story under Parkfield earthquake: **a** displacement; **b** control force

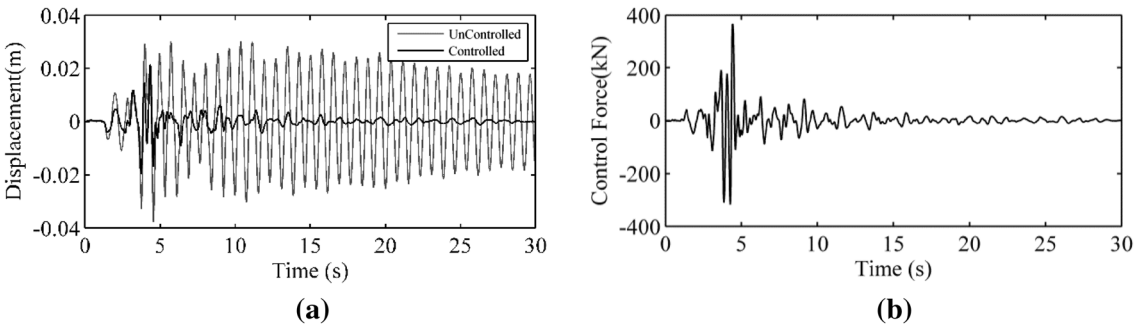

Fig. 18 The results of FA controller for 8-dof top story under Parkfield earthquake: **a** displacement; **b** control force

Table 16 Comparison between the FA and LQR for 3-dof under Parkfield earthquake

	J	Dispmax (m)	Velmax (m/s)	Accmax (m/s^2)	Umax (kN)	Driftmax
UC	–	0.0544	0.8403	13.3886	–	0.00352
LQR	0.5793	0.0269	0.4847	7.4851	2.2456	0.00211
FA	0.4477	0.0257	0.4611	7.2971	1.8251	0.00206

Table 17 Comparison between FA and LQR for 8-dof under Parkfield earthquake

	J	Dispmax (m)	Velmax (m/s)	Accmax (m/s^2)	Umax (kN)	Driftmax
UC	0	0.0375	0.4303	7.3899	0	0.0011
LQR	1.2295	0.0205	0.2326	4.5455	576.798	0.0005
FA	1.2324	0.0212	0.2801	6.0198	365.714	0.0007

Harmony Search Algorithm

Begin
*Objective function f(**x**), **x** = $(x_1, ..., x_d)^T$;*
Generate initial harmonics (real number arrays)
Define pitch adjusting rate (r_{pa}). pitch limits and bandwidth (BW)
Define harmony memory accepting rate (r_{accept})
***while** (t<Max number of iterations)*
Generate new harmonics by accepting best harmonics
Adjust pitch to get new harmonics (solutions)
***if** (rand> r_{accept}, choose an existing harmonic randomly*
***else if** (rand> r_{pa}), adjust the pitch randomly within limits*
***else** generate new harmonics via randomization*
end if
Accept the new harmonics if better
end while
Find the current best solutions
Post process results and visualization;
End

Fig. 19 The pseudo-code of HS

Table 18 The values of HS parameters

Bandwidth	BW	0.2
Harmony memory choosing rate	HMCR	0.95
Pitch adjust rate	PAR	0.3

4.7 Comparison of six studied metaheuristics in active control of structures

In this section, the results of six previously introduced optimal controllers are compared. To gain accurate comparison, fixed parameters are used for all algorithms including population size and iteration number. The iteration number for all methods is set as 50. The initial population sizes of all algorithms for 3- and 8-dof structures are set to 30 and 50. The summarized result of all algorithms for 3-dof structure against Kobe earthquake is drawn in Table 21.

The effectiveness of these controllers in reducing the response of the three-story building due to Landers and Parkfield earthquake is also shown in Tables 22, 23.

According to Table 21, the response reduction ratio (ratio of the controlled to uncontrolled response) at top floor of 3-dof shear frame against Kobe earthquake is about 78%, 77%, 77%, 78%, 76% and 78% for ICA, DE, BAT, BEE, FA and HS controllers, respectively. This decrement is about 11%, 9%, 9%, 10%, 5% and 13% compared to LQR, aligned with other similar earthquakes. Comparison between the metaheuristics and LQR for 8-dof structure under Parkfield earthquake is drawn in Table 24.

The response reduction ratio at top story of 8-dof structure against Parkfield earthquake is about 46%, 45%, 47%, 46%, 43% and 46% for ICA, DE, BAT, BEE, FA and HS controllers. Almost the same behavior is observed for other earthquakes as well. Consequently, the metaheuristics performance is more optimal than LQR controller; therefore, the maximum response of structure and needed control force are reduced compared to LQR.

Also, the comparison of benchmark indices has provided the appropriate information about the advantages of designed controllers. The values of these indices for 3-dof under Parkfield earthquake are shown in Table 25. Based on the calculations, all controllers have performed better than LQR; however, ICA controller performance is optimal than others.

Regarding other comparative criterion, the root mean square (RMS) of responses is used, accordingly, the results

Table 19 Comparison between HS and LQR for 3-dof under Kobe earthquake

	J	Dispmax (m)	Velmax (m/s)	Accmax (m/s^2)	Umax (kN)	Driftmax
UC	–	0.0658	0.9369	15.7387	–	0.0047
LQR	0.4956	0.0164	0.2573	5.377	2.164	0.0014
HS	0.4667	0.0143	0.2352	5.1215	1.922	0.0013

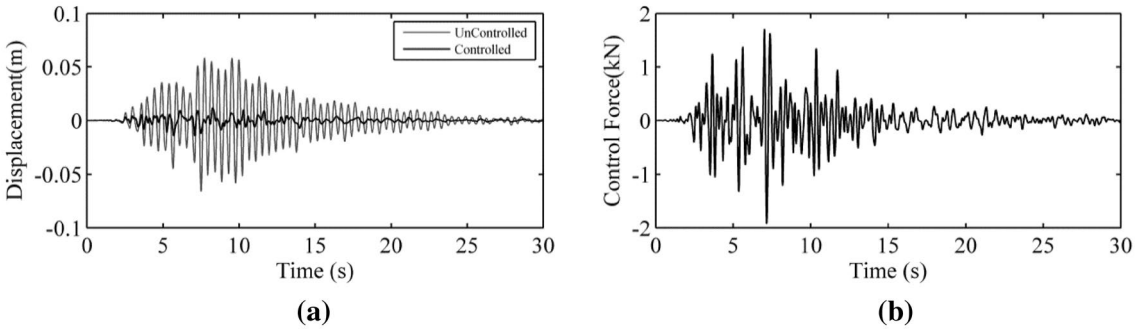

Fig. 20 HS controller results for 3-dof top story under Kobe earthquake: **a** displacement; **b** control force

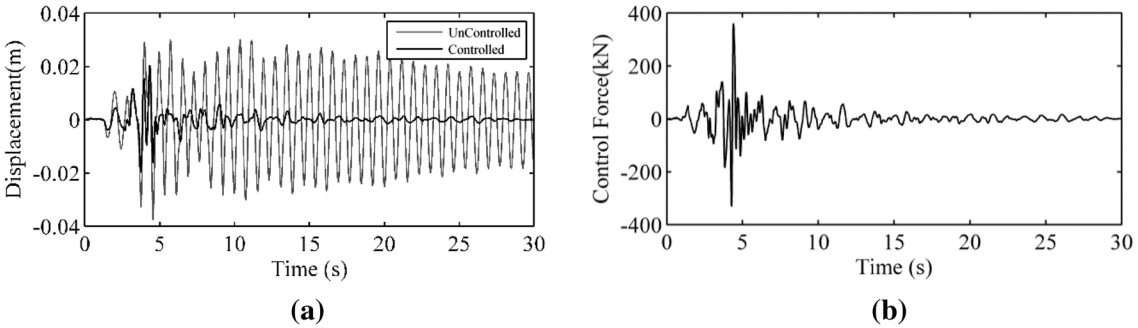

Fig. 21 HS controller results for 8-dof top story under Parkfield earthquake: **a** displacement; **b** control force

Table 20 The comparison between HS and LQR for 8-dof under Parkfield earthquake

	J	Dispmax (m)	Velmax (m/s)	Accmax (m/s^2)	Umax (kN)	Driftmax
UC	–	0.0355	0.4303	7.3899	–	0.00217
LQR	1.2295	0.02051	0.2326	4.5455	576.7981	0.00133
HS	1.2120	0.02033	0.2735	5.8072	360.9319	0.00217

Table 21 Comparison between the metaheuristics and LQR for 3-dof under Kobe earthquake

	J	Dispmax (m)	Velmax (m/s)	Accmax(m/s^2)	Umax (kN)	Driftmax
UC	–	0.0658	0.9369	15.7387	–	0.0047
LQR	0.4956	0.0164	0.2573	5.377	2.164	0.0014
ICA	0.4384	0.0146	0.2208	4.7267	1.982	0.0012
DE	0.4488	0.015	0.2354	5.0676	2.004	0.0013
BAT	0.4536	0.015	0.2164	4.9023	2.136	0.0013
BEE	0.4677	0.0148	0.2399	5.2675	1.858	0.0014
FA	0.4676	0.0155	0.2456	5.3502	2.06	0.0015
HS	0.4667	0.0143	0.2352	5.1215	1.922	0.0013

of RMS of displacement for 3-dof under Parkfield earthquake are shown in Fig. 22.

The numerical analysis of the above RMS curves has shown total RMS of displacement response (total area in RMS curve) for ICA, DE, BAT, BEE, FA and HS as 23%, 25%, 23%, 23%, 25% and 25% of total RMS of displacement for LQR controller. This percentage is about 83%, 91%, 86%, 85%, 93% and 93% of total RMS of uncontrolled displacement showing ICA's performance more optimal than other metaheuristics. RMS of needed control force for 8-dof shear frame under Parkfield is shown in Fig. 23.

Table 22 Comparison between the metaheuristics and LQR for 3-dof under Landers earthquake

	J	Dispmax (m)	Velmax (m/s)	Accmax (m/s^2)	Umax (kN)	Driftmax
UC	–	0.0354	0.4424	6.8714	–	0.0024
LQR	0.3248	0.0189	0.1771	2.2658	1.125	0.0011
ICA	0.2793	0.0168	0.1811	2.6094	0.764	0.0011
DE	0.28	0.0168	0.1784	2.6674	0.72	0.0011
BAT	0.2999	0.017	0.1786	2.6591	0.773	0.0011
BEE	0.2827	0.0165	0.178	2.6529	0.771	0.0011
FA	0.3012	0.0172	0.191	2.8775	0.78	0.0011
HS	0.3008	0.0175	0.1877	2.8231	0.792	0.0011

Table 23 Comparison between the metaheuristics and LQR for 3-dof under Parkfield earthquake

	J	Dispmax (m)	Velmax (m/s)	Accmax (m/s^2)	Umax (kN)	Driftmax
UC	–	0.0544	0.8403	13.3886	–	0.0035
LQR	0.5793	0.0269	0.4847	7.4851	2.246	0.0021
ICA	0.4264	0.0237	0.4204	6.7744	1.818	0.002
DE	0.4374	0.0254	0.4569	7.3248	1.524	0.0021
BAT	0.4416	0.0239	0.4378	7.0013	1.722	0.0019
BEE	0.4347	0.0237	0.432	6.9661	1.646	0.0019
FA	0.4477	0.0257	0.4611	7.2971	1.825	0.0021
HS	0.4393	0.026	0.4589	7.2669	1.628	0.0021

Table 24 Comparison between the metaheuristics and LQR for 8-dof under Parkfield earthquake

	J	Dispmax (m)	Velmax (m/s)	Accmax (m/s^2)	Umax (kN)	Driftmax
UC	0	0.0375	0.4303	7.3899	0	0.0011
LQR	1.2295	0.0205	0.2326	4.5455	576.798	0.0005
ICA	1.0794	0.0203	0.2708	5.5173	285.469	0.0006
DE	1.1781	0.0205	0.2834	5.8792	312.167	0.0007
BAT	1.1993	0.0198	0.2717	5.8573	427.913	0.0007
BEE	1.2895	0.0203	0.2852	6.1476	453.94	0.0007
FA	1.2324	0.0212	0.2801	6.0198	365.714	0.0007
HS	1.212	0.0203	0.2735	5.8072	360.932	0.0007

Table 25 The results of benchmark indices for 3-dof under Parkfield earthquake

	LQR	ICA	DE	BAT	BEE	FA	HS
J_1	0.4773	0.3946	0.4375	0.4045	0.4149	0.4393	0.441
J_2	0.4861	0.4213	0.4553	0.4293	0.4269	0.4602	0.464
J_3	0.5591	0.506	0.5471	0.5229	0.5203	0.545	0.5428
J_4	0.5882	0.0002	0.0003	0.0004	0.0005	0.0003	0.0073
J_5	0.2175	0.1794	0.1966	0.1845	0.1834	0.1997	0.2008
J_6	0.2354	0.1956	0.2143	0.2013	0.2003	0.2181	0.2188
J_7	0.2727	0.2366	0.2555	0.2425	0.2436	0.2595	0.2601
J_8	0.2682	2.31×10^{-05}	3.13×10^{-05}	4.96×10^{-05}	4.84×10^{-05}	3.90×10^{-05}	0.0008
J_9	0.0763	0.0618	0.0586	0.062	0.0559	0.062	0.0553

According to Fig. 23, the total RMS of control force (the covered area of RMS curve) calculated by ICA method is 52% of control force needed for LQR. This percentage for DE, BAT, BEE, FA and HS is 55%, 75%, 70%, 61% and 55%; subsequently, ICA's performance is also better than other techniques. The convergence rate has significantly determined the comparison of metaheuristics observed and compared from Fig. 24 for 8-dof under Parkfield earthquake.

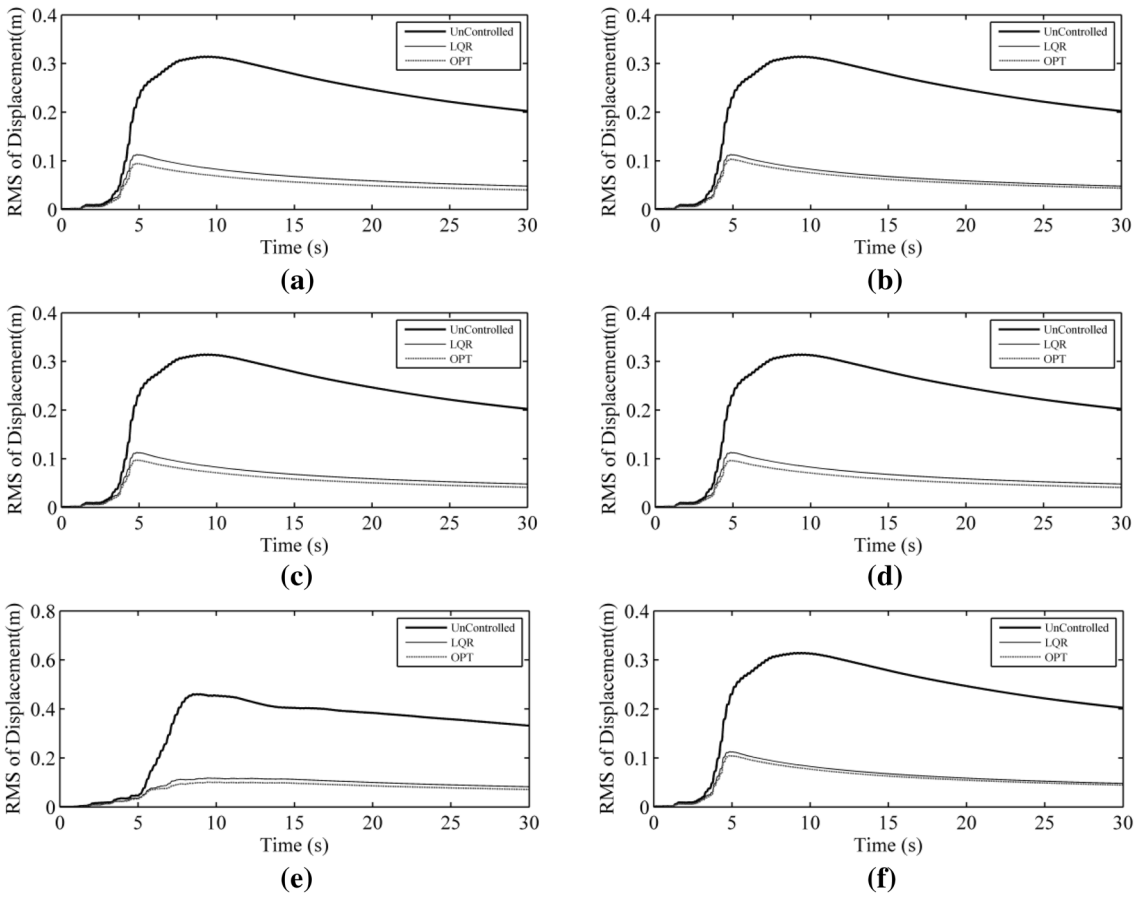

Fig. 22 RMS of 3-dof top story displacement under Parkfield earthquake: **a** ICA; **b** DE; **c** BAT; **d** BEE; **e** FA; **f** HS controllers

Similar behavior has been repeated for 3-dof convergence under various earthquakes showing the out performs of ICA than other methods in terms of convergence rate, respectively, DE and BAT are located in other next ranks.

5 Conclusions

The current study has focused on an optimal configuration of LQR controller applied on 3-dof and 8-dof structures subjected to several historical earthquakes. Based on the results, the metaheuristic optimizer has made control system meet optimal states and control energy, simultaneously. Due to the multiplicity of metaheuristics, the optimization objective function has been performed by six methods and the results have been compared to one another.

- Computational time is an important characteristic of optimization algorithm. Regarding the whole processing time (from the initial to the final configuration), the comparisons have revealed a faster run in HS (50 iterations in about 1 min), also, ICA and DE have required slightly more time than HS; however, BAT and FA are weaker and BEE is the slowest algorithm (4–5 times slower than ICA).
- Considering Fig. 24, FA and BAT have good convergence tendency compared to other algorithms (convergence occurred in about 10 iterations) as a favorable choice for computational burden reduction, meanwhile, the convergence occurred for ICA, DE and BEE is about 40 iterations. Subsequently, regarding the convergence rate, the mentioned metaheuristics have been ranked as FA (first rank) and BAT, ICA, DE and BEE (the next).
- Considering total cost value, ICA and DE have produced better results compared to all the mentioned algorithms. BAT, HS, BEE and FA have second, third, fourth, fifth and sixth rank. Additionally, all the mentioned algorithms have produced better results than LQR. Consequently, each metaheuristic algorithm has advantages and disadvantages in solving active control problem; furthermore, considering the effectiveness of six intelligent controllers, ICA, DE, and HS have performed favorably for the very optimization problem in

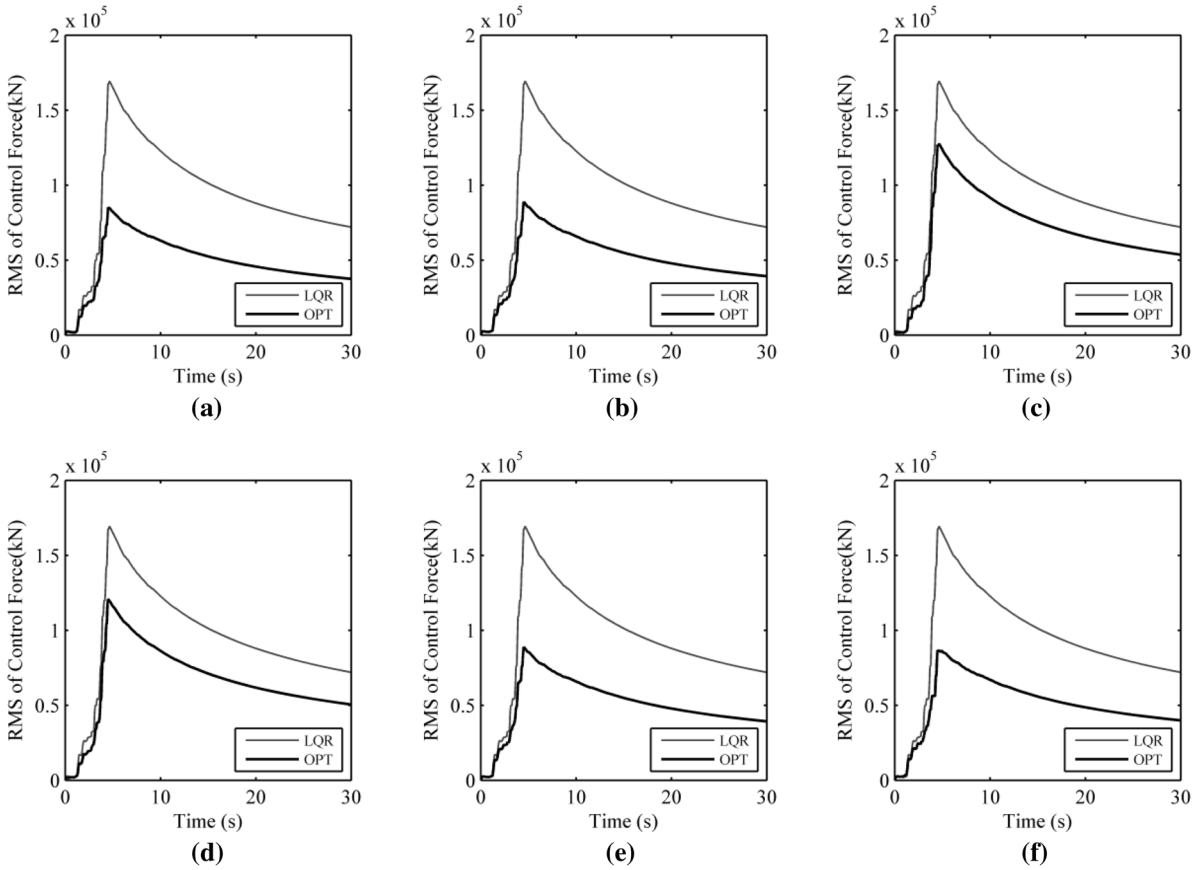

Fig. 23 RMS of control force for 8-dof under Parkfield earthquake: **a** ICA; **b** DE; **c** BAT; **d** BEE; **e** FA; **f** HS controllers

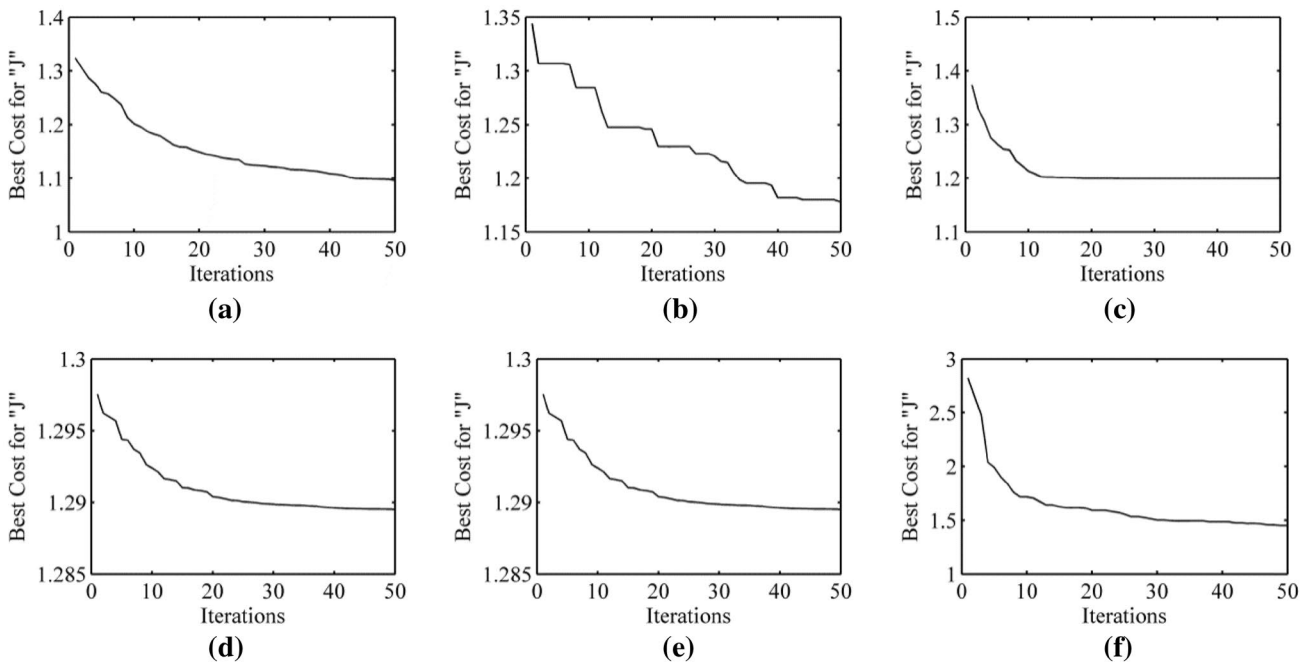

Fig. 24 Convergence rate of all algorithms for 8-dof under Parkfield earthquakes: **a** ICA; **b** DE; **c** BAT; **d** BEE; **e** FA; **f** HS controllers

seeking of the best solution, convergence rate and computational effort. On the contrary, BAT, FA, and BEE have been weakly performed for the problems and leveled the next. The superiority of ICA over other methods in finding the optimal responses for active control problem has been shown as well.

To sum up, the results for active control of structures have shown the potential of wavelet and metaheuristic algorithms in vibration control for building structures depending on the user to select the appropriate algorithm or on the problem types and its requirements such as the quality of solution, convergence rate, computational effort, and consuming time.

References

1. Ali Toghroli et al (2014) Prediction of shear capacity of channel shear connectors using the ANFIS model. Steel Compos Struct 17(5):623–639
2. Safa M et al (2016) Potential of adaptive neuro fuzzy inference system for evaluating the factors affecting steel-concrete composite beam's shear strength. Steel Compos Struct Int J 21(3):679–688
3. Mohammadhassani M et al (2015) Fuzzy modelling approach for shear strength prediction of RC deep beams. Smart Struct Syst 16(3):497–519
4. Mansouri I et al (2017) Analysis of influential factors for predicting the shear strength of a V-shaped angle shear connector in composite beams using an adaptive neuro-fuzzy technique. J Intell Manuf 1–11
5. Toghroli A (2015) Applications of the ANFIS and LR models in the prediction of shear connection in composite beams. Jabatan Kejuruteraan Awam, Fakulti Kejuruteraan, Universiti Malaya
6. Aghakhani M et al (2015) A simple modification of homotopy perturbation method for the solution of Blasius equation in semi-infinite domains. Math Prob Eng 2015:7
7. Toghroli A et al (2016) Potential of soft computing approach for evaluating the factors affecting the capacity of steel–concrete composite beam. J Intell Manuf 29:1–9
8. Sadeghipour Chahnasir E et al (2018) Application of support vector machine with firefly algorithm for investigation of the factors affecting the shear strength of angle shear connectors. Smart Struct Syst 22(4):413–424
9. Safa M et al (2016) Potential of adaptive neuro fuzzy inference system for evaluating the factors affecting steel–concrete composite beam's shear strength. Steel Compos Struct 21(3):679–688
10. Mansouri I et al (2016) Strength prediction of rotary brace damper using MLR and MARS. Struct Eng Mech 60(3):471–488
11. Toghroli A et al (2018) Evaluation of the parameters affecting the Schmidt rebound hammer reading using ANFIS method. Comput Concr 21(5):525–530
12. Sari PA, et al (2018) An intelligent based-model role to simulate the factor of safe slope by support vector regression. Eng Comput
13. Sedghi Y et al (2018) Application of ANFIS technique on performance of C and L shaped angle shear connectors. Smart Struct Syst 22(3):335–340
14. Shariat M, Shariati M (2018) Computational Lagrangian multiplier method by using for optimization and sensitivity analysis of rectangular reinforced concrete beams. Steel Compos Struct 29:243–256
15. Grandhi RV (1990) Optimum design of space structures with active and passive damping. Eng Comput 6(3):177–183
16. Hadi MN, Uz ME (2015) Investigating the optimal passive and active vibration controls of adjacent buildings based on performance indices using genetic algorithms. Eng Optim 47(2):265–286
17. Amini F, Tavassoli MR (2005) Optimal structural active control force, number and placement of controllers. Eng Struct 27(9):1306–1316
18. Datta T (2003) A state-of-the-art review on active control of structures. ISET J Earthq Technol 40(1):1–17
19. Elseaidy WM, Baugh JW, Cleaveland R (1996) Verification of an active control system using temporal process algebra. Eng Comput 12(1):46–61
20. Liu J, Wang Y (2008) Design approach of weighting matrices for LQR based on multi-objective evolution algorithm. In: 2008 International conference on information and automation (ICIA). IEEE, Changsha, China, pp 1188–1192
21. Wang W et al (2012) Weight optimization for LQG controller based on the artificial bee colony algorithm. AASRI Procedia 3:686–693
22. Wang H, et al (2013) Optimization of LQR controller for inverted pendulum system with artificial bee colony algorithm. In: Proceedings of the 2013 international conference on advanced mechatronic systems 2013. IEEE, Louyang, China, pp 158–162
23. Bottura CP, da Fonseca Neto J (1999) Parallel eigenstructure assignment via LQR design and genetic algorithms. In: Proceedings of the 1999 American control conference. IEEE, San Diego, CA, USA
24. Bottura CP, da Fonseca Neto JV (2000) Rule-based decision-making unit for eigenstructure assignment via parallel genetic algorithm and LQR designs. In: Proceedings of the 2000 American control conference. IEEE, Chicago, IL, USA
25. Shen P (2014) Application of genetic algorithm optimization LQR weighting matrices control inverted pendulum. Appl Mech Mater 543–547:1274–1277
26. Joghataie A, Mohebbi M (2012) Optimal control of nonlinear frames by Newmark and distributed genetic algorithms. Structl Des Tall Spec Build 21(2):77–95
27. Petković D, Ćojbašič Ž, Nikolić V (2013) Adaptive neuro-fuzzy approach for wind turbine power coefficient estimation. Renew Sustain Energy Rev 28:191–195
28. Petković D et al (2014) Adaptive neuro-fuzzy maximal power extraction of wind turbine with continuously variable transmission. Energy 64:868–874
29. Petković D et al (2014) Adapting project management method and ANFIS strategy for variables selection and analyzing wind turbine wake effect. Nat Hazards 74(2):463–475
30. Nikoli V et al (2017) Wind speed parameters sensitivity analysis based on fractals and neuro-fuzzy selection technique. Knowl Inf Syst 52(1):255–265
31. Petković D, Pavlović NT, Ćojbašić Ž (2016) Wind farm efficiency by adaptive neuro-fuzzy strategy. Int J Electr Power Energy Syst 81:215–221
32. Bishop J, Striz A (2004) On using genetic algorithms for optimum damper placement in space trusses. Struct Multidiscip Optim 28(2–3):136–145
33. Singh MP, Moreschi LM (2002) Optimal placement of dampers for passive response control. Earthq Eng Struct Dyn 31(4):955–976
34. Cha Y-J et al (2012) Multi-objective genetic algorithms for cost-effective distributions of actuators and sensors in large structures. Expert Syst Appl 39(9):7822–7833

35. Amini F, Hazaveh NK, Rad AA (2013) Wavelet PSO-based LQR algorithm for optimal structural control using active tuned mass dampers. Comput-Aid Civ Infrastruct Eng 28(7):542–557
36. Aghajanian S et al (2014) Optimal control of steel structures by improved particle swarm. Int J Steel Struct 14(2):223–230
37. Amini F, Ghaderi P (2012) Optimal locations for MR dampers in civil structures using improved Ant Colony algorithm. Opt Control Appl Methods 33(2):232–248
38. Bekdaş G, Nigdeli SM (2011) Estimating optimum parameters of tuned mass dampers using harmony search. Eng Struct 33(9):2716–2723
39. Amini F, Ghaderi P (2013) Hybridization of harmony search and ant colony optimization for optimal locating of structural dampers. Appl Soft Comput 13(5):2272–2280
40. Aydin E (2012) Optimal damper placement based on base moment in steel building frames. J Constr Steel Res 79:216–225
41. Mohebbi M, Joghataie A (2012) Designing optimal tuned mass dampers for nonlinear frames by distributed genetic algorithms. Struct Des Tall Spec Build 21(1):57–76
42. Zarbaf SEHAM et al (2017) Stay cable tension estimation of cable-stayed bridges using genetic algorithm and particle swarm optimization. J Bridge Eng 22(10):05017008
43. Chen X et al (2018) Prediction of shear strength for squat RC walls using a hybrid ANN–PSO model. Eng Comput 34(2):367–383
44. Tian H, Shu J, Han L (2018) The effect of ICA and PSO on ANN results in approximating elasticity modulus of rock material. Eng Comput 35:1–10
45. Sierra MR, Coello CAC (2005) Improving PSO-based multi-objective optimization using crowding, mutation and ∈-dominance. In: International conference on evolutionary multi-criterion optimization. Springer, New York
46. Leung A, Zhang H (2009) Particle swarm optimization of tuned mass dampers. Eng Struct 31(3):715–728
47. Özsarıyıldız ŞS, Bozer A (2015) Finding optimal parameters of tuned mass dampers. Struct Des Tall Spec Build 24(6):461–475
48. Bagheri A, Amini F (2013) Control of structures under uniform hazard earthquake excitation via wavelet analysis and pattern search method. Struct Control Health Monit 20(5):671–685
49. Amini F, Bagheri A (2014) Optimal control of structures under earthquake excitation based on the colonial competitive algorithm. Struct Des Tall Spec Build 23(7):500–511
50. Gandomi AH, Yang X-S, Alavi AH (2013) Cuckoo search algorithm: a metaheuristic approach to solve structural optimization problems. Eng Comput 29(1):17–35
51. Yang X-S (2010) A new metaheuristic bat-inspired algorithm. In: Nature inspired cooperative strategies for optimization (NICSO 2010). Springer, New York, pp 65–74
52. Varaee H, Ghasemi MR (2017) Engineering optimization based on ideal gas molecular movement algorithm. Eng Comput 33(1):71–93
53. Ghasemi MR, Varaee H (2017) A fast multi-objective optimization using an efficient ideal gas molecular moment algorithm. Eng Comput 33(3):477–496
54. Gendreau M, Potvin J-Y (2010) Handbook of metaheuristics, vol 2. Springer, New York
55. Yang X-S (2013) Multiobjective firefly algorithm for continuous optimization. Eng Comput 29(2):175–184
56. Ohtori Y et al (2004) Benchmark control problems for seismically excited nonlinear buildings. J Eng Mech 130(4):366–385
57. Atashpaz-Gargari E, Lucas C (2007) Imperialist competitive algorithm: an algorithm for optimization inspired by imperialistic competition. In: 2007 IEEE Congress on evolutionary computation (CEC). IEEE, Singapore, pp 4661–4667
58. Storn R, Price K (1997) Differential evolution–a simple and efficient heuristic for global optimization over continuous spaces. J Glob Optim 11(4):341–359
59. Pham D, et al (2005) The bees algorithm. Technical note. Manufacturing Engineering Centre, Cardiff University, UK, pp 1–57
60. Yang X-S (2008) Firefly algorithm. In: Nature-inspired metaheuristic algorithms. Luniver Press, pp 79–90
61. Geem ZW, Kim JH, Loganathan G (2001) A new heuristic optimization algorithm: harmony search. Simulation 76(2):60–68